J. Plasma Fusion Res. SERIES, Vol.7 (2006) 110-113

Monte Carlo Simulation of Cylindrical Langmuir Probe Sheaths

GOTO Makoto, KONDOH Yoshiomi[1], SHENG Min[1], TAKAHASHI Toshiki[1],
IWASAWA Naotaka[1] and OKADA Tomio[2]

Kanto Polytechnic College, Oyama 323-0813, Japan

[1] *Gunma University, Kiryu 376-8515, Japan*

[2] *Maebashi Institute of Technology, Maebashi 371-0816, Japan*

(Received: 5 October 2004 / Accepted: 21 december 2005)

Abstract

A self-consistent Monte Carlo modeling technique has been developed to study the sheath structure and property of cylindrical Langmuir probes. The introduced technique takes into account low-density and high-energy particles as well as enables the reduction of the calculation time of excitation collision cross sections. The electron and ion current-voltage characteristics show good agreement with the probe theory and experimental results. The sheath structure and wide-range electron energy distributions are shown. The sweep time dependence on current-voltage characteristics is explained by the structure.

Keywords:

Monte Carlo simulation, cylindrical Langmuir probe, current-voltage characteristic, sheath structure, electron energy distribution

1. Introduction

An electric probe referred to as the Langmuir probe is commonly used to diagnose plasma parameters (*e.g.*, electron temperature) for steady state, isotropic, and unmagnetized plasmas. Besides the measurement of quiet plasmas, the requirement for observing the plasma parameters of RF glow discharges for etching, sputtering, and CVD applications have increased recently. This is due to the increasing role of plasma processing in modern technologies. The results of simulation studies on RF glow discharges satisfactorily predict the experimental characteristics and provide useful information such as the spatial variation of plasma parameters in sheaths and plasma and their temporal evolutions.

This study is a benchmark to confirm that the simulation results show good agreement with the experimental current-voltage characteristics of the Langmuir probe because it is established that the requirement for further applications of simulation codes is inevitable. In the present study, the particle simulations are carried out for the cylindrical Langmuir probe in argon plasma. A fine subslab technique and the weight probability method are used [1, 2] and modified particularly in the plasma source region (object of measurements) so that high-energy particles are generated and simulated over a simulation space and time. Furthermore, some new techniques are introduced in order to reduce the calculation time.

The obtained electron current-voltage characteristics are in good agreement with the Langmuir probe theory and experiments. The electron current shows an exponential curve over three orders in the simulation results of a Maxwellian plasma source using 2000 particles in a ring slab. The electron energy distributions are obtained within a range of over four orders of magnitude. The spatial variations of the electron and ion densities and potential are shown, and the difference in the ion sheath and electron sheath is clarified. The sweep time dependence on current-voltage characteristics is explained by the structure.

2. Simulation model and method

An infinitely long cylindrical Langmuir probe with radius r_i (0.5 mm) is considered to be in the center of an infinitely long cylindrical argon plasma with radius r_o (5.5 mm), as shown in Fig. 1. The probe potential V_p with respect to the plasma end is swept from −5 V to 2 V and from 2 V to −5 V with speeds of 0.025 V/μ s and 0.2 V/μ s. The simulation particles of the electrons and ions (Ar^+) are traced under the influence of a radial self-consistent electric field recalculated at the end of every time step. The time interval dT_s for the calculation of the electric field is 1.0 ns.

The simulation space is divided into M_m (= 50) ring slabs. A ring slab is divided into 10 subslabs. The

Corresponding author's e-mail: goto@oyama-pc.ac.jp

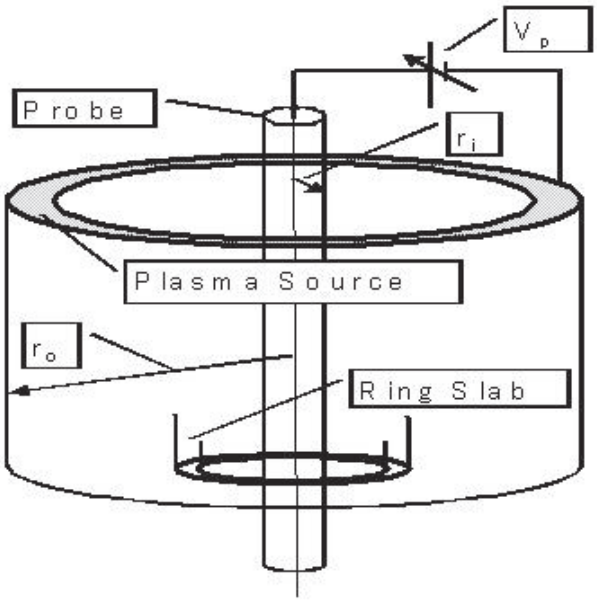

Fig. 1 Schematic of structure and circuit of simulation model.

space resolution is restricted due to the separation of subslabs. The weight probability method and fine subslab system are used [1, 2]. Thus, all the simulation particles have not only three-dimensional positions and velocities but also individual weights. The standard particle number N_s of any electron and ion in a ring slab is 2000. The plasma source consists of two outer ring slabs and three neighboring ring slabs. The test particles in the two outer ring slabs are supplied (renewed) during each dT_s. The plasma source density N_p is set at $1.0 \times 10^{16}\,\mathrm{m}^{-3}$, and the electron energy kT_e and ion energy kT_i of the two outer ring slabs are 2/3 eV and 1/37 eV, respectively, where k, T_e, and T_i are the Boltzmann constant, electron temperature, and ion temperature, respectively.

At the end of every time step, the new electron velocities of the two outer ring slabs are determined by random values between 0 and $4(kT_e/m)^{1/2}$, where m is the mass of an electron. The weights of the simulation particles are calculated under the condition that the velocity distribution is Maxwellian and density is N_p. Thus, a sufficient number of high-energy electrons can be simulated. In this procedure, the highest energy of an electron is below the ionization energy. Thus, the ionization collisions are negligibly small. On the other hand, the ion velocities of the two outer ring slabs are randomly selected from a group of 10000 velocities that comprise the Maxwell distribution. Both the outer ring slabs have equal ion weights. The electron and ion weights in the three neighboring ring slabs of the two outer ring slabs are regulated at the end of every time step in order to maintain a constant plasma density N_p.

The radial electric field E_r is calculated self-consistently from the charge density distribution ρ by using the following equation:

$$E_r = \frac{1}{r}\left[\frac{1}{\varepsilon_0}\left\{\int_{r_i}^{r}\rho\xi d\xi - \frac{1}{\ln(r_0/r_i)}\int_{r_i}^{r_0}\rho\xi\ln\left(\frac{r_0}{\xi}\right)d\xi\right\} + \frac{V_p}{\ln(r_0/r_i)}\right], \tag{1}$$

where ε_0 is the permittivity in vacuum.

The electron collisions (elastic, excitation, and ionization) and ion collisions (elastic and charge exchange) are considered only in neutral argon gas. The electron and ion collision cross sections that are used are provided by the JILA of Colorado University [3].

In order to reduce the calculation time of the excitation collision procedure, we introduced a combined cross-section system. We combined 25 excitation collision cross sections $Q_i(U)$ with 25 different threshold energies U_i of argon. The combined excitation cross section $Q_{ex}(U)$ and energy loss function $E_{loss}(U)$ for an electron with kinetic energy U are calculated as follows:

$$Q_{ex}(U) = \sum_{i=1}^{25} Q_i(U), \tag{2}$$

$$E_{loss}(U) = \sum_{i=1}^{25} Q_i(U)\cdot U_i \Big/ \sum_{i=1}^{25} Q_i(U). \tag{3}$$

By using the combined cross-section system and energy loss function, we can reduce the time required to accurately calculate the electron energy after many excitation collisions in a statistical manner.

The ion and electron simulation times are individually set, as shown in Fig. 2. The acceleration factor A_c is introduced to reduce the calculation time. In every time step dT_s, ions are simulated throughout; however, electrons are simulated only during dT_s/A_c. The dT_s is determined such that the ion plasma oscillation time is longer than dT_s and the change in ion density in dT_s is small. The electron simulation time dT_s/A_c is determined such that the electron plasma oscillation

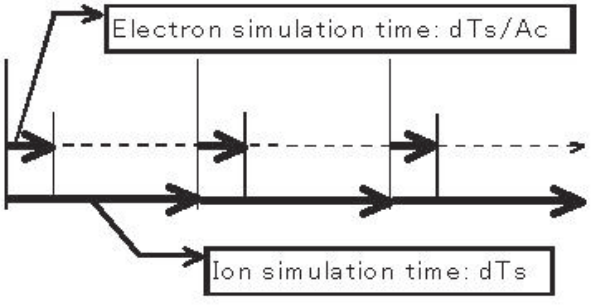

Fig. 2 Time flow chart of electron and ion simulation.

time exceeds dT_s/A_c, and the motion of electrons during dT_s/A_c is faster than that of the ions during dT_s. Our simulations are performed under the condition that no ionization collision occurs. We obtain the electron current by multiplying the electron charge flow in the probe during dT_s/A_c by A_c. When A_c is below 2000, it is confirmed that the current-voltage characteristics are in good agreement with the Langmuir probe theory and experiments. In this study, A_c is equal to 500.

3. Results and discussion

We first tested the simulation code for a quasi-ideal condition. Figure 3 shows the voltage characteristics of the electron and ion current densities under low argon pressure (reduced pressure $p_0 = 13.3$ Pa). Figure 3 shows the two types of sweep directions. The increasing and decreasing probe potential are swept at the same speed 0.025 V/μs. These two curves are almost in good agreement. For this condition, the mean free path of the electrons and ions are 19 mm and 0.38 mm, respectively, and the Debye length is 0.06 mm. In this case, it is considered that the sheath is thin and does not undergo collision. The electron energy kT_e obtained from the electron current curve shown in Fig. 3 is 0.67 eV. The plasma density obtained from the electron saturation current is 1.0×10^{16} m^{-3}. These are in good agreement with a parameter of the plasma source. The obtained floating potential is -3.4 V, and the ratio of the saturation currents between electrons and ions is around 200. These are almost in agreement with the value calculated from the Bohm criterion. These results may provide some amount of evidence for validating this simulation.

The ion current appears to be somewhat small, especially in the low negative- and zero-voltage regions. It seems that ion current decay with a low negative probe potential is primarily due to the collision of ions and also the growth of a thin and weak reverse field surrounding the probe surface to a certain extent. It is confirmed that the ion current decreases significantly as the gas pressure increases. For the ions, there exists a potential wall with a value of around $-kT_i$ when V_p is 0 V. Although this may require more precise consideration, it beyond the scope of this study.

Figure 4 shows the current density characteristics at a sweep speed of 0.2 V/μs. These curves exhibit hysteresis characteristics. The electron current for a decreasing sweep voltage from 0 V to -1 V tends to remain at the saturation value. The two ion current curves are different over a wide range. The ion current for the decreasing voltage is less than that for the increasing voltage near a space potential. The relation varies inversely over a deep negative probe potential. These may be explained qualitatively by considering the density distributions and mass of charged particles.

The radial distributions of the plasma parameters are obtained in the simulation shown in Fig. 3. We present some typical results of the simulation. Figure 5 shows the potential distributions of four probe potentials (-5, -2, 0, and 2 V). Figures 6 and 7 show the distributions of electron density N_e and ion density N_i, respectively. All the results for this situation contain spatiotemporal fluctuations. For example, the space potential in the plasma region varies with a magnitude of around kT_e. The time averaged value is considered.

The negative probe potential have a long-range influence up to the plasma source. When a negative potential is applied, there is a growth in a wide sheath and pre-sheath. In the long-range pre-sheath, this weak field accelerates the ions. In order to sustain an effectively

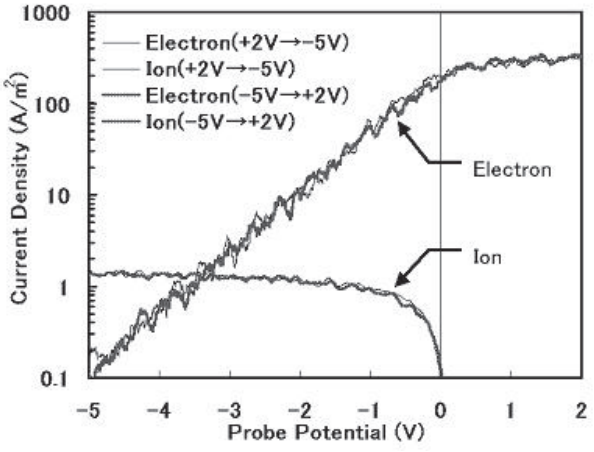

Fig. 3 Electron and ion current density characteristics at a sweep speed of 0.025 V/μs.

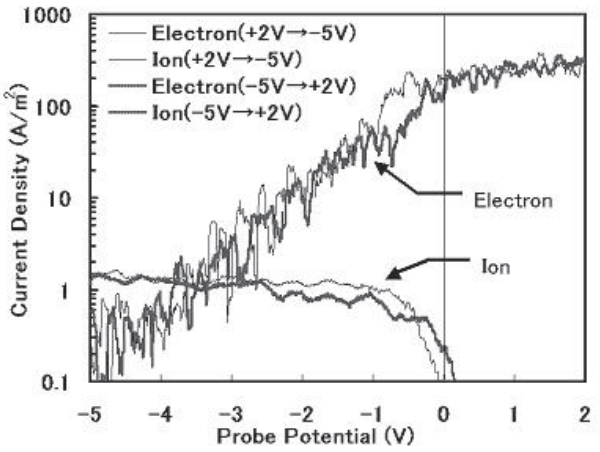

Fig. 4 Electron and ion current density characteristics at a sweep speed of 0.2 V/μs.

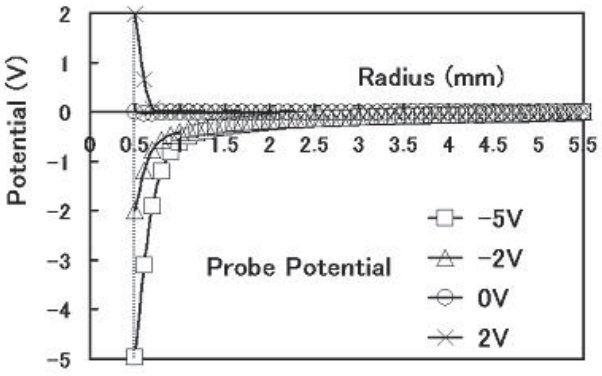

Fig. 5 Potential distributions.

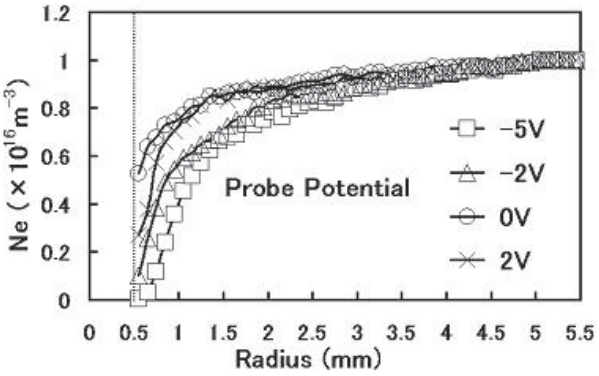

Fig. 6 Electron density distributions.

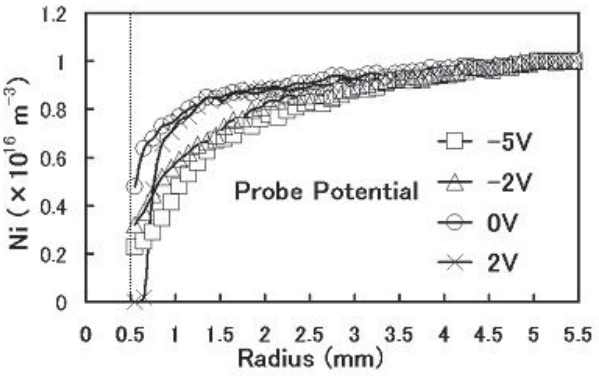

Fig. 7 Ion density distributions.

large ion flow, not only diffusion flow but also drift flow is required in the plasma. The electric field for gathering ions is governed by the electrons. The field is controlled within a value where electrons play the role of charge neutrality. On the other hand, the positive potential is perfectly shielded within a short region. When the probe potential is positive or zero, the sheath is narrow and prevents plasma density decay near the sheath. When the ion current is low or zero, a very weak field can compensate the ion diffusion of the density gradient. The electrons are accelerated by a positive potential through the short region. These are verified from the mean energy distributions of the electrons and ions.

The features comprise the wide sheath and pre-

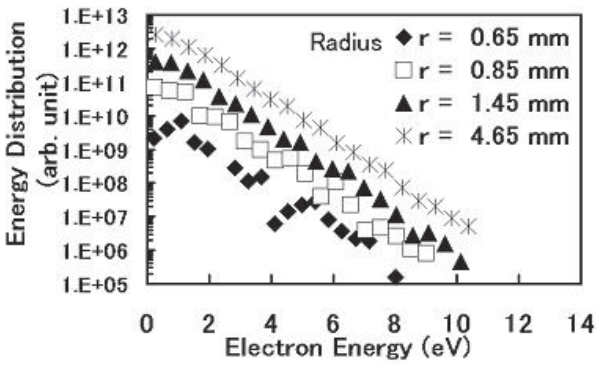

Fig. 8 Electric energy distributions at $V_p = -5$ V.

sheath obtained at a negative probe voltage, while a positive voltage leads to the shallow sheath and prevents plasma density decay. A high plasma density near the probe causes high electron and ion currents beginning from the positive probe potential; however, a large mass of ions leads to a delay in the increase of ion current, thereby resulting in the hysteresis curve shown in Fig. 4.

The electron energy distributions of four positions at a negative potential ($V_p = -5$ V) are shown in Fig. 8. The wide-energy distributions (over four orders of magnitude) are obtained. By employing the weight probability method, the supplied energy distribution in the plasma source has a wide range. Furthermore, the energy loss due to a collision is negligibly small. Thus, the Boltzmann relation is confirmed, as shown in Fig. 8. On the other hand, the ion distributions in the sheath are not Maxwellian. The accelerated ions have wider band distributions.

4. Concluding remarks

A cylindrical Langmuir probe simulation has been developed. The fine subslab technique and weight probability method are used and modified particularly in the plasma source region. A combined cross section system is introduced to reduce the simulation time. The obtained electron and ion current-voltage characteristics show good agreement with the probe theory and experimental results. The profiles of the potential and electron and ion densities are clarified, and wide-range electron energy distributions are shown.

References

[1] M. Goto *et al.*, Jpn. J. Appl. Phys. **36**, 4815 (1997).

[2] M. Goto and Y. Kondoh, Jpn. J. Appl. Phys. **37**, 308 (1998).

[3] JILA of Colorado Univ. home page: jilawww.colorado.edu/research/colldata.html.